A Prediction of Thermal Stress Profiles in the Steam Turbine Startup Phase Using Fourier Neural Operator

So Jung Lee[1], Hwan In Oh[1], Dong Hwan Kim[2] , Myoung Soo Park[2], and Joon Ha Jung[1]

[1]*Department of Industrial Engineering, Ajou University, Suwon, Gyeonggi-do, 16499, Republic of Korea*
judy0807@ajou.ac.kr
ohhi0928@ajou.ac.kr
joonha@ajou.ac.kr

[2]*KEPCO Research Institute, Daejeon, 34056, Republic of Korea*
astronaut83@naver.com
msmspark@gmail.com

ABSTRACT

Frequent startup and shutdown of steam turbines in recent operations have increased the importance of analyzing thermal stress induced by rapid temperature changes. In turbine startup, particularly during the synchronization phase, the surface temperature rises sharply while the core temperature lags behind, creating thermal gradients that lead to stress accumulation. However, the limited availability of measured data during these transient intervals poses a significant challenge for data-driven temperature prediction models, which typically require large-scale training datasets.

To address this issue, we propose a Fourier Neural Operator (FNO)-based framework to predict four temperature sequences during the synchronization phase using limited warm and hot startup data. The input consists of statistical features derived from two temperature-related and two steam-related variables observed during the preceding 3000 RPM holding phase. To ensure temporal consistency, all samples are padded to a unified sequence length.

The proposed FNO architecture leverages spectral convolution to capture global dependencies while maintaining local temporal resolution. Comparative evaluations with CNN, DNN, and LSTM models under identical training conditions demonstrate that the FNO consistently achieves higher predictive accuracy and robustness in five-fold cross-validation. These results indicate that the FNO-based framework is well-suited for modeling thermal dynamics in transient turbine operations where high-resolution data is scarce.

*Corresponding Author: Joon Ha Jung (joonha@ajou.ac.kr)

1. INTRODUCTION

Thermal stress is a critical factor in determining the structural integrity and operational reliability of steam turbines, especially during transient phases such as grid synchronization. Rapid changes in temperature and load during this phase can induce stress concentrations that significantly impact component fatigue life and maintenance schedules. Accurate prediction of thermal stress profiles during these dynamic intervals is thus essential for safe and efficient turbine operation.

Steam turbines frequently undergo repeated start-up and shut-down cycles due to flexible power grid demands and economic load dispatching. These repetitive thermal loadings introduce significant thermal fatigue and stress accumulation in critical components. However, the limited availability of operational data during turbine start-up phases restricts the applicability of conventional deep learning methods, which typically require large datasets to generalize effectively. This challenge underscores the need for a data-efficient and physics-consistent modeling approach that can perform reliably even with limited data available in turbine start-up phases.

During rapid operational transitions such as turbine startup, significant temperature differences often arise due to the differing thermal responses of turbine components. While the surface temperature of the rotor increases rapidly in response to external heat, the temperature of the core region increases more slowly. This imbalance induces considerable thermal stress across the structure. If both surface temperature and the resulting thermal stress can be accurately predicted, it becomes possible to optimize startup

control strategies, extend the lifespan of the turbine, and improve overall power generation efficiency.

Using the Fourier Neural Operator (FNO), we propose a prediction model for forecasting temperature profiles during the grid connection interval of steam turbine startup. The model takes as input a combination of temperature and steam-related variables observed during the prior 3000 RPM holding phase, and predicts the temporal evolution of multiple temperature targets. By learning from real-world operational data, the proposed FNO-based approach eliminates the need for computationally expensive simulations while maintaining physical consistency, offering a practical solution for temperature forecasting in data-scarce turbine start-up conditions.

2. BACKGROUND

2.1. Neural Operator

A Neural Operator is a class of models designed to learn mappings between infinite-dimensional function spaces. Unlike traditional architectures that process finite-dimensional input vectors, Neural Operators directly learn the relationship between input and output functions defined over continuous domains. Given an input function $a(x) \in A$, the goal is to approximate an operator G such that $G(a) \approx u$, where $u(x) \in U$ is the corresponding output function.

To enable learning in function space, Neural Operators parameterize the mapping via integral kernel operations and function-valued weights, allowing for generalization across different input domains and boundary conditions. This function-level abstraction allows Neural Operators to capture complex physical relationships and dynamic behaviors that vary not just across data points, but across entire function distributions.

Neural Operators are particularly well-suited for modeling physical systems governed by partial differential equations (PDEs), where the underlying processes are naturally described in terms of spatial and temporal functions. Their ability to learn operators, rather than pointwise mappings, enables them to generalize beyond training data and handle previously unseen conditions in a mathematically coherent way.

2.2. Fourier Neural Operator

The architecture of the Fourier Neural Operator (FNO) consists of three principal components: the Lifting Layer, a series of Fourier Layers, and the Projection Layer. These components enable the transformation of low-dimensional input functions into a high-dimensional spectral space, the learning of global interactions in frequency space, and the reconstruction of target outputs.

Lifting Layer:

The input function : $u(x) \in \mathbb{R}^d$, defined over a spatial or temporal domain Ω, is first embedded into a higher-dimensional space using a learned pointwise linear transformation:

$$v^0(x) = P_{lift}(u(x)) \in \mathbb{R}^C,$$

where $C \gg d$. This expansion allows the model to represent richer latent structures suitable for Fourier-based operations.

Fourier Layer:

The lifted representation is then passed through multiple spectral convolution layers. Each Fourier layer updates the hidden representation $v^{(\ell)}$ by applying a nonlocal transformation:

$$v^{(\ell+1)}(x) = \sigma(Wv^{(\ell)}(x) + \mathcal{F}^{-1}(R^{(\ell)} \cdot \mathcal{F}(v^{(\ell)}))(x),$$

where $\mathcal{F}$ and $\mathcal{F}^{-1}$ are the Fourier and inverse Fourier transforms, $R^{(\ell)}$ is a learnable filter in Fourier space, and σ is a nonlinear activation function such as GELU. These layers enable the model to learn global patterns and long-range dependencies in a resolution-invariant manner.

Projection Layer:

Finally, the output of the last Fourier layer $v^{(L)}(x)$ is mapped back to the original output dimension through a linear projection:

$$\hat{u}^{\theta}(x) = P_{proj}(v^{(L)}(x)) \in \mathbb{R}^m,$$

where m is the dimensionality of the target output. This step compresses the high-dimensional latent representation into the desired prediction space.

3. DATA DESCRIPTION

3.1. Operating Regimes and Startup Phase Composition

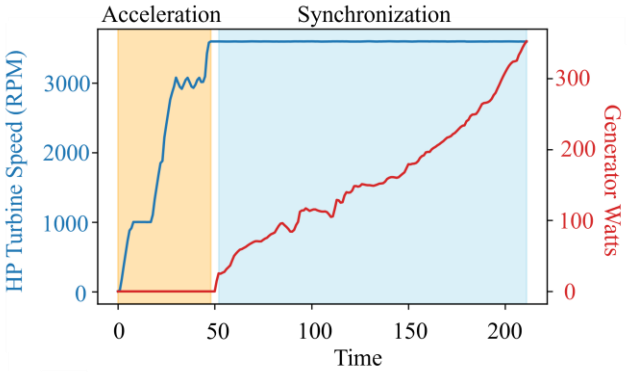

Figure 1. Acceleration and Synchronization Phases During Warm and Hot/Restart Startup Operations

Steam turbine startup operations are typically categorized into three regimes based on the initial rotor temperature: cold, warm, and hot/restart. Each startup sequence consists

of multiple phases, including preheating, acceleration, and generator synchronization.

The preheating phase is only present in cold startups, during which the turbine remains inactive for an extended period and must be gradually warmed before rotation begins. In contrast, the acceleration phase, where rotor speed increases from 0 to the rated 3600 RPM, and the synchronization phase, during which generator load is applied after reaching rated speed, are common to all startup types.

In this study, we focus exclusively on warm and hot/restart startups, which do not include the preheating phase. Among the segments in these startups, two intervals are of particular interest: the 3000 RPM holding phase and the generator synchronization phase. The 3000 RPM holding phase refers to a short period within the acceleration phase where turbine speed stabilizes around 3000 RPM after a rapid increase. The synchronization phase follows, marked by a rapid rise in generator load, causing steep changes in temperature and thermal stress that significantly influence structural integrity.

These two phases—3000 RPM holding and synchronization—are shown in Figure 1. The orange-shaded region illustrates the acceleration phase, including the 3000 RPM holding period, while the blue-shaded region represents the synchronization phase where load application begins. Reflecting the physical significance of these intervals, we use the 3000 RPM holding phase as the input segment and the synchronization phase as the prediction target in our modeling framework.

Table 1. Data Description.

Variable name	Description
HP Turbine Surface Temperature	Temperature measured at the outer surface of the high-pressure turbine casing.
HP Turbine Bore Temperature	Temperature measured at the bore of the high-pressure turbine rotor.
IP Turbine Surface Temperature	Temperature measured at the outer surface of the intermediate-pressure turbine.
IP Turbine Bore Temperature	Temperature measured at the bore of the intermediate-pressure turbine.
Main Steam Pressure	Pressure of the main steam supplied to the turbine inlet.
Reheat Steam Temperature	Temperature of the steam after being reheated between turbine stages.

3.2. Variable Selection

A total of six variables were selected for model development, considering both their thermal relevance and their availability from sensor measurements during turbine startup. These variables encompass the surface and bore (core) temperatures of the high-pressure (HP) and intermediate-pressure (IP) turbines, as well as the main steam and reheat steam temperatures.

Among these, the HP and IP surface temperatures, along with the main and reheat steam temperatures, are used as model inputs. The outputs of the model are defined as the surface and bore temperatures of both the HP and IP turbines, reflecting the internal thermal state of the system. This configuration is particularly useful for stress-related prediction tasks, as bore temperature estimation is often critical yet difficult to measure directly in practice.

A detailed description of the selected variables and their physical meaning is summarized in Table 1. For example, the HP Turbine Surface Temperature refers to the temperature measured at the outer casing of the high-pressure turbine, while the HP Bore Temperature represents internal measurements at the rotor core. These physically interpretable variables ensure that the modeling approach is aligned with the underlying thermal and mechanical processes during turbine startup.

4. PROPOSED METHOD

4.1. Input Feature Construction and Preprocessing

To construct structured inputs for the Fourier Neural Operator (FNO), raw sensor measurements from the 3000 RPM holding phase are transformed into compact temporal descriptors. Four physical variables are selected: HP turbine surface temperature, IP turbine surface temperature, main steam temperature, and reheat steam temperature.

For each variable, three descriptive features—initial value, final value, and linear slope—are computed over the holding interval, resulting in a 12-dimensional input vector for each startup instance. These features are chosen to effectively represent thermal behavior without depending on high-resolution time-series data. The initial and final values capture the thermal boundary states, while the slope accounts for the rate of change, which is particularly important when sequence durations vary and thermal gradients intensify over longer intervals.

A normalized time variable t is appended to form a 13-dimensional input. This composite input is passed through a

learnable embedding layer that projects it onto a 4-dimensional latent space suitable for spectral learning.

Since the length of the holding phase varies across startup samples, all sequences are padded to match the maximum observed length. This padding is essential because the FNO requires inputs of consistent temporal dimension to perform global spectral transformations. By enforcing uniform sequence lengths, stable model training and effective generalization across samples are ensured.

In parallel, the local branch applies a pointwise linear transformation in the spatial domain using a separate set of learnable weights. This branch ensures that fine-grained local variations in the data are preserved, which might otherwise be smoothed out during global spectral operations.

The outputs from both global and local branches are combined element-wise and passed through a nonlinear activation function. This fusion allows the network to learn both broad trends and local fluctuations, which is essential for accurate modeling of dynamic physical processes such as turbine temperature evolution.

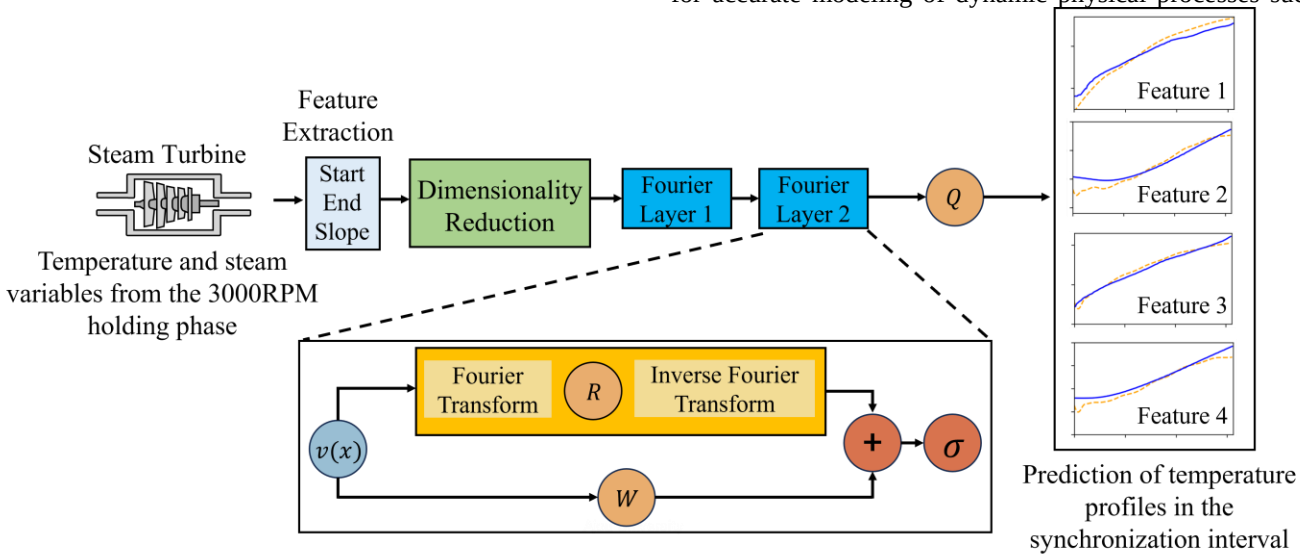

Figure 2. Architecture of the Fourier Neural Operator (FNO) Model

4.2. Fourier Neural Operator Architecture

The Fourier Neural Operator (FNO) employed in this study is designed to model physical systems by leveraging both global and local information from the input data. The overall architecture comprises three key components: a lifting layer, Fourier layers, and a projection layer. The structure is illustrated in Figure 2.

First, the lifting layer transforms the structured input vector into a high-dimensional latent representation through a pointwise neural operation. This process enables the model to embed low-dimensional statistical features—such as initial value, final value, and slope—into a richer representation space suitable for spectral learning.

Next, the Fourier layers perform two types of operations in parallel: global and local processing. In the global branch, the high-dimensional input undergoes a Fast Fourier Transform (FFT), is multiplied by learnable complex-valued weights in the frequency domain, and is then transformed back to the spatial domain via inverse FFT. This operation allows the model to capture long-range dependencies and global patterns across time and variables.

Finally, the projection layer maps the high-dimensional output into the final prediction space, producing the four target temperature sequences during the synchronization phase.

5. RESULTS

To evaluate the effectiveness of the proposed FNO-based prediction framework, we compared its performance against three representative deep learning architectures: Convolutional Neural Network (CNN), Deep Neural Network (DNN), and Long Short-Term Memory (LSTM). All models were trained using the same input features, target variables, loss function, and 5-fold cross-validation setup to ensure a fair comparison.

Figure 3 illustrates the prediction performance of each model using a representative fold, visualized through line plots for all four target temperature variables: HP turbine surface temperature, HP turbine bore temperature, RH turbine surface temperature, and RH turbine bore temperature. These line plots directly compare the actual temperature profiles and the predicted values from each model. The FNO model achieved the closest match to the

actual data across all variables, especially during periods of rapid change. CNN and DNN, in contrast, exhibited substantial prediction errors, particularly in regions of high thermal variation. LSTM provided moderately accurate predictions but still failed to match the precision of FNO.

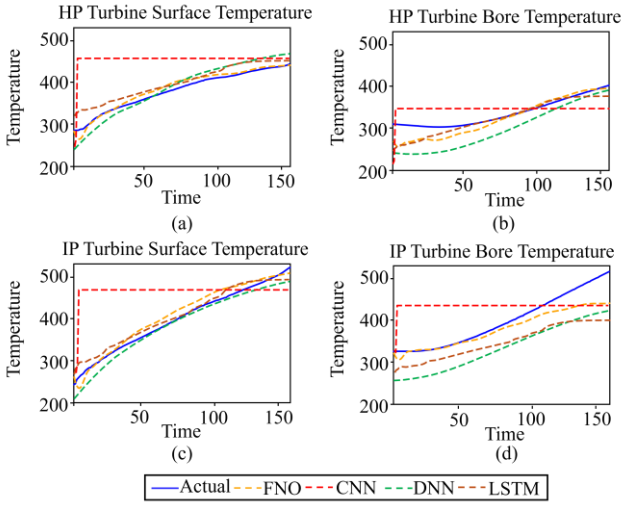

Figure 3. Model Comparison on Fold 4: Predicted vs. Actual Temperature Profiles

Figure 4 presents the quantitative comparison of model performance through R^2 scores across all five folds. The error bars indicate the standard deviation of performance across folds. The FNO model consistently outperformed the other models, maintaining an average R^2 above 0.9 and demonstrating both high accuracy and stability. CNN showed the poorest performance, with R^2 scores close to zero and large variability. DNN and LSTM achieved intermediate results but lacked consistency across different folds.

The fold-wise prediction performance for each model on each target temperature variable is detailed in Tables 2 through 5, corresponding respectively to the HP turbine surface temperature, HP turbine bore temperature, RH turbine surface temperature, and RH turbine bore temperature. These tables confirm the superior and stable generalization ability of the FNO model across all cases.

6. CONCLUSIONS

In this study, we proposed a Fourier Neural Operator (FNO)-based framework to predict temperature evolution in the synchronization phase of steam turbine startup, focusing on data-limited warm and hot start conditions. Unlike conventional equation-based thermal analysis methods, which often suffer from accuracy limitations due to discrepancies between modeling assumptions and actual measurements, the proposed data-driven approach leverages temporal and spectral learning to improve prediction fidelity.

We constructed the model using four input variables—two temperature-related and two steam-related—derived

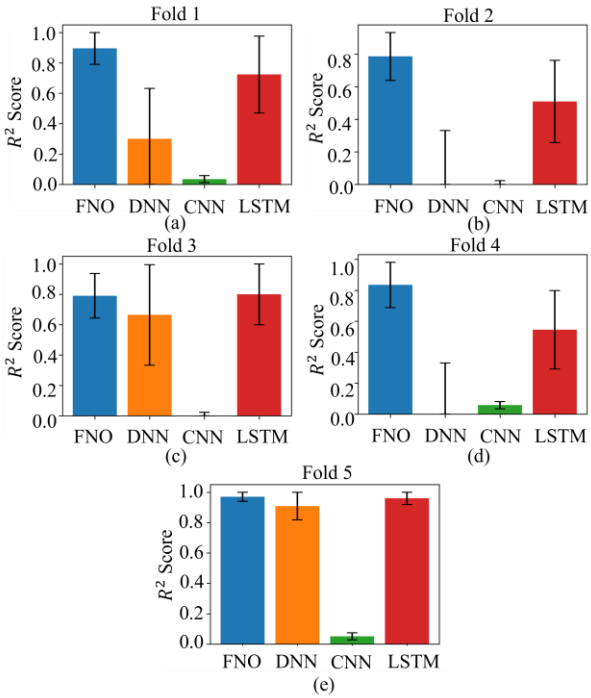

Figure 4. Error Bar Graphs Showing R^2 Score Variability Across Five-Fold Cross-Validation for All Models

Table 2. R^2 Score for HP Turbine Surface Temperature

	Accuracy			
Fold	FNO	DNN	CNN	LSTM
1	0.8732	0.6562	0.1043	0.8712
2	0.9380	0.8642	0.0119	0.8017
3	0.9674	0.8987	0.0518	0.8915
4	0.9627	0.9113	0.0511	0.8479
5	0.8733	0.7027	0.0525	0.8706

Table 3. R^2 Score for HP Turbine Bore Temperature

	Accuracy			
Fold	FNO	DNN	CNN	LSTM
1	0.9528	0.8143	0.0069	0.9168
2	0.9159	0.8974	0.0015	0.9628
3	0.8700	0.6963	0.0314	0.8449
4	0.9379	0.5115	0.0187	0.8791
5	0.4559	0.4423	0.0080	0.4475

from the 3000 RPM holding region. These were transformed into temporal features such as initial value, final value, and slope. The model then predicted four target temperature profiles during the subsequent synchronization phase. To ensure temporal uniformity, all samples were padded to match the maximum length across start-up instances.

Comprehensive comparisons with baseline models (CNN, DNN, LSTM) under identical training settings revealed that the FNO model significantly outperformed others, achieving the highest R^2 scores and demonstrating robustness across multiple folds. The results underscore the FNO's capability to capture both global and local thermal patterns effectively, even under sparse and non-periodic industrial time-series data.

The proposed FNO framework is expected to provide a robust foundation for real-time thermal monitoring and control of power generation systems, particularly in transient regimes where physical modeling is difficult or incomplete.

Table 4. R^2 Score for IP Turbine Surface Temperature

	Accuracy			
Fold	FNO	DNN	CNN	LSTM
1	0.9620	0.7635	0.0627	0.9508
2	0.9575	0.8308	0.0211	0.7788
3	0.9673	0.8358	0.0542	0.9350
4	0.9680	0.9380	0.0416	0.9388
5	0.9108	0.8185	0.0052	0.8344

Table 5. R^2 Score for IP Turbine Bore Temperature

	Accuracy			
Fold	FNO	DNN	CNN	LSTM
1	0.9651	0.6155	0.0250	0.9579
2	0.9563	0.9541	0.0145	0.9261
3	0.8787	0.4900	0.0030	0.8152
4	0.9134	0.1331	0.0237	0.6874
5	0.1369	0.1279	0.0364	0.0038

ACKNOWLEDGEMENT

The acknowledgement section is optional. Please list any acknowledgment here using a single paragraph.

REFERENCES

Li, Z., Kovachki, N., Azizzadenesheli, K., Liu, B., Bhattacharya, K., Stuart, A., & Anandkumar, A. (2020). Fourier neural operator for parametric partial differential equations. arXiv preprint arXiv:2010.08895.

Goswami, S., Bora, A., Yu, Y., & Karniadakis, G. E. (2023). Physics-informed deep neural operator networks. In Machine learning in modeling and simulation: methods and applications (pp. 219-254). Cham: Springer International Publishing.

BIOGRAPHIES

So Jung Lee is currently pursuing a Master's degree in Industrial Engineering at Ajou University. She holds a BSc in Industrial Engineering from Ajou University, which she obtained in 2024. Her primary research focus is on predicting the remaining useful life (RUL) of bearings based on physical knowledge transfer methods. She is also engaged in research activities related to RUL prediction and fault diagnosis of machinery at the Data Intelligent PHM Lab at Ajou University.

Hwan In Oh is currently pursuing his Master's degree in Industrial Engineering at Ajou University. He holds a BSc in Industrial Engineering from Ajou University, which he obtained in 2024. Prior to beginning his graduate studies, he worked as a researcher at the Korea Electronics Technology Institute (KETI). His primary research focus is on fault diagnosis for rotating machinery using zero-shot learning. He is also engaged in research activities related to fault diagnosis and anomaly detection for rotating machinery at the Data Intelligent PHM Lab at Ajou University.

Myoung Soo Park is working at the KEPCO Research Institute, focusing on the operation and maintenance of thermal power plants.

Dong Hwan Kim is working at the KEPCO Research Institute, focusing on the operation and maintenance of thermal power plants.

Joon Ha Jung is currently serving as an assistant professor of industrial engineering at Ajou University. He holds a BSc and a PhD in mechanical engineering from Seoul National University, which he obtained in 2012 and 2019, respectively. Prior to joining Ajou University, he worked as a senior researcher at the Korea Institute of Machinery and Materials (KIMM). Professor Jung's primary research focus is on fault diagnosis for rotating machinery, and he is also engaged in research activities that uses machine learning and deep learning.

APPENDIX

If the paper has an appendix, the appendix should appear at the end of the paper after the biographies. The appendix section is optional.